ELSEVIER

Chemical Engineering Journal 91 (2003) 205–213

Chemical Engineering Journal

www.elsevier.com/locate/cej

Modeling of critical phenomena for liquid/vapor–gas exothermic reaction on a single catalyst pellet

A.B. Shigarov, A.V. Kulikov, N.A. Kuzin, V.A. Kirillov*

Boreskov Institute of Catalysis, Prosp. Akad. Lavrentieva 5, 630090 Novosibirsk, Russia

Abstract

Physical mechanisms are discussed and crude mathematical models with lumped parameters are developed, which explain the authors recent experimental data [4], concerning temperature hysteresis and multiplicity phenomena for α-methylstyrene (AMS) liquid–vapor hydrogenation on a single catalyst pellet. The interplay between endothermic vaporization and exothermic vapor phase reaction is elucidated. The results of this study may help to develop more sophisticated models and theory of hot spots formation and runaway phenomena in trickle-bed reactors.

Keywords: Modeling; Hydrocarbons hydrogenation; Single pellet multiphase reactor; Runaway; Partial wetting; Evaporation; Hysteresis

1. Introduction

The essential part of industrial multiphase (gas–liquid–solid) heterogeneous catalytic reactions is carried out in the trickle-bed adiabatic reactors. These reactions may be rather exothermic and volatility of the liquid phase may be also noticeable. A typical example of such reactions is hydrogenation of hydrocarbons. So far, the problem, attracting both the academician and industrial interest is how to escape hot spots (resulting in low selectivity, coking, sintering and runaway) and meanwhile to keep productivity of the trickle-bed reactor. The challenging task is to understand the intrinsic mechanism for transition from the well-known normal trickling operation (liquid phase reaction on the internally liquid filled catalyst) to the abnormal one (gas phase reaction with vaporization on partially dry pellets). The experimental investigations of α-methylstyrene (AMS) [1] and cyclohexene [2] hydrogenation in a laboratory trickle-bed reactor revealed hysteresis and multiplicity of steady states and the impact of vaporization, gas phase reaction and liquid distribution. Unfortunately, no models were suggested because the local picture was unclear. Study [3] was the first to establish multiplicity for cyclohexene hydrogenation on pellet scale, though only for the case when the gas flow contained no vapor and the liquid flow rate was constant. Experimental research [4] has pointed out the impact of the combined evaporation of the liquid phase and gas phase reaction on single catalyst pellet performance. The exothermic, catalyzed hydrogenation of α-methylstyrene (AMS) to cumene has been employed as a model reaction. Steady state and dynamic experiments have been performed in a single catalytic pellet reactor using five catalytic pellets of different porous structures, thermal conductivity, apparent catalytic activity and distribution of catalyst in the pellet. Gas phase temperature, concentration of AMS in the gas phase and the liquid flow rates have been varied. The measured center and surface temperatures of each pellet reveal hysteresis phenomena with a varying liquid flow rate on a single catalyst pellet and the existence of two significantly different steady states in the range of liquid flow rate. The range of the liquid flow rate over which the two steady states were observed, the pellet temperature and the pellet dynamics depend strongly on the amount of AMS vapor in the gas phase and the catalyst properties. Theoretical studies concerning this item are rather scarce. A mathematical model of the half-side wetted and partially liquid filled catalyst slab was developed [5], but it was not compared with experimental data. Both the theoretical and experimental study of the gas phase hydrogenation of hydrocarbons on the dry catalyst pellet under external transport control of reaction rate [6] partially elucidates the earlier obtained experimental data. The goal of this study was to suggest physical and mathematical models for understanding of critical phenomena, which have been experimentally observed for the AMS hydrogenation on the partially wetted catalyst pellet [4]. Although our attempts to suggest a universal model to explain all the experimental data were not successful, we consider two rather crude

* Corresponding author. Tel.: +7-3832-341187; fax: +7-3832-341187.
E-mail address: v.a.kirillov@catalysis.nsk.su (V.A. Kirillov).

1385-8947/02/$ – see front matter © 2002 Elsevier Science B.V. All rights reserved.
PII: S1385-8947(02)00155-9

Nomenclature

C	molar concentration of AMS vapor (mol/m^3)
c_A	heat capacity of AMS (J/(mol K))
d	pellet diameter (m)
D_A	coefficient of pseudo binary diffusion for AMS vapor (m^2/s)
D_{AB}	coefficient of binary diffusion for AMS and cumene vapor (m^2/s)
D_{AH}	coefficient of binary diffusion for AMS vapor and hydrogen (m^2/s)
D_{ef}	effective coefficient of vapor diffusion in porous layer (m^2/s)
E	activation energy for gas phase reaction (J/mol)
f	fraction of wet external surface of catalyst pellet
G_{AMS}	liquid AMS mass flow rate (kg/s)
h_{dry}	thickness of dry layer (m)
h_{wet}	layer thickness, necessary for complete AMS vapor conversion (m)
H_{ev}	heat effect of AMS evaporation (J/mol)
M	molar mass (kg/mol)
N_{AMS}	liquid AMS molar flow rate (mol/s)
k_i	catalytic activity constant (mol/(m^3 s Pa$^{0.8}$))
P	total pressure (N/m^2)
P_H	partial pressure of hydrogen (N/m^2)
P_{vap}	partial pressure of saturated AMS vapor (N/m^2)
r	intrinsic kinetic rate of AMS gas phase hydrogenation (mol/(s m^3))
R	ideal gas constant (J/(mol K))
S	external area of catalyst pellet (m^2)
T	pellet temperature (C or K)
I_0	gas flow temperature (C or K)
Q_p	heat effect of AMS hydrogenation reaction (J/mol)
W_{reac}	total rate of AMS vapor hydrogenation (mol/s)
W_{ev}	total rate of AMS evaporation (mol/s)
x	molar fraction of gas flow components
X	AMS vapor conversion

Greek symbols

α	gas–solid heat transfer coefficient (W/(m^2 K))
α_{int}	intra pellet heat transfer coefficient (W/(m^2 K))
β	gas–solid mass transfer coefficient (m/s)
ε	porosity of catalyst pellet
λ	coefficient of gas phase heat conductivity (W/(m K))
λ_p	coefficient of pellet heat conductivity (W/(m K))
τ	tortosity of catalyst pellet

Dimensionless numbers

Nu	Nusselt number
Pr	Prandtl number
Re	Reynolds number
Sc	Schmidt number
Sh	Sherwood number

Subscripts

A	α-methylstyrene (AMS)
B	cumene
dry	dry external surface of pellet
H	hydrogen
s	pellet surface
wet	wet external surface of pellet

but essentially nonlinear mathematical models with lumped parameters, corresponding to different gas flow composition. These models are based on the different physical assumptions, corresponding to different gas flow composition (hydrogen, saturated by AMS vapor or not). The first model (gas flow: $A_{vap} + H_2$) assumes that both evaporation and gas phase reaction zones are spatially divided and they take place consequently on wet and dry parts of catalyst pellet external surface under gas–solid interphase mass transfer rate control. So, heat transfer across the pellet (from one zone to another) via thermal conductivity plays crucial role in this case and 2T-model is necessary. The second model (gas flow: H_2) assumes that evaporation and gas phase reaction zones are in close contact and are placed inside a pellet. The rate of reaction is controlled by the rate of evaporation, and the last is defined by internal diffusion of vapors with H_2 in subsurface porous layer, which divides external pellet surface and intra pellet evaporation front. Spherical symmetry is assumed and, therefore, 1T-model is valid. Finally, detailed comparison of experimental data [4] with the results of modeling is done.

2. Case of hydrogen flow, saturated by AMS vapor

2.1. Physical assumptions

Here we consider the so called "hot" catalyst pellet steady state (or higher branch) (Fig. 1). Hydrogen flow is saturated by AMS vapor (which is generated in the separate evaporator upstream) under constant flow temperature and streams around the pellet. Liquid AMS (having the same temperature) is fed to the top of the pellet. The upper part of the external pellet surface is wet. All liquid is evaporated from this area under gas–solid interphase mass transfer rate control. Evaporation from the wet surface to the saturated gas flow is possible because the wet surface has higher temperature than gas. The last effect is explained by heat transfer from the dry and relatively hot part of the pellet

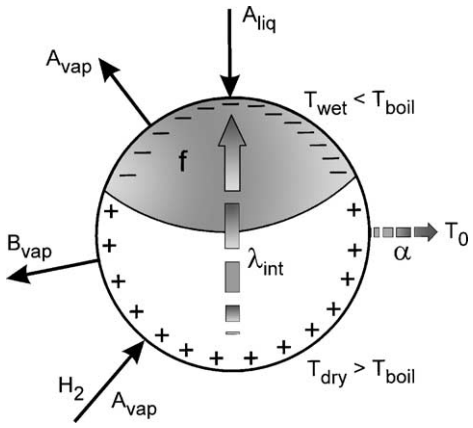

Fig. 1. Hypothetical catalyst pellet upper branch steady state in case of hydrogen flow, saturated by AMS vapor.

external surface to the wet one via pellet thermal conductivity. Gas phase AMS hydrogenation occurs on the dry pellet surface under gas–solid interphase mass transfer rate control. Thus, we assume that exothermic reaction and corresponding flow-pellet temperature rise are provided exclusively by AMS vapor from streaming gas, but not by AMS vapor, which is generated on the wet pellet surface and which is simply blown away with the following vapor condensation in the downstream saturated to equilibrium gas.

2.2. Mathematical model of steady states

Heat balance for the dry part of the external surface:

$$\beta_{\mathrm{dry}}(1-f)C_0Q_{\mathrm{p}} = \alpha(1-f)(T_{\mathrm{dry}}-T_0) + \alpha_{\mathrm{int}}f(T_{\mathrm{dry}}-T_{\mathrm{wet}}) \quad (1)$$

Heat balance for the wet part of the external surface:

$$\alpha_{\mathrm{int}}(T_{\mathrm{dry}}-T_{\mathrm{wet}}) = \beta_{\mathrm{wet}}(C-C_0)(H_{\mathrm{ev}}+c_{\mathrm{A}}(T_{\mathrm{wet}}-T_0)) + \alpha(T_{\mathrm{wet}}-T_0) \quad (2)$$

Material balance for liquid AMS:

$$N_{\mathrm{AMS}} = \beta_{\mathrm{wet}}Sf(C-C_0); \qquad N_{\mathrm{AMS}} = \frac{G_{\mathrm{AMS}}}{M_{\mathrm{AMS}}} \quad (3)$$

$$C_0 = \frac{P_{\mathrm{vap}}(T_0)}{RT_0}; \qquad C = \frac{P_{\mathrm{vap}}(T_{\mathrm{wet}})}{RT_{\mathrm{wet}}};$$
$$P_{\mathrm{vap}} = P^*\exp\left(\frac{-H_{\mathrm{ev}}}{RT}\right) \quad (4)$$

$$\alpha = \frac{Nu\lambda}{d}; \qquad \beta_{\mathrm{wet}} = \frac{D_{\mathrm{AH}}Sh(D_{\mathrm{AH}})}{d};$$
$$\beta_{\mathrm{dry}} = \frac{D_{\mathrm{A}}Sh(D_{\mathrm{A}})}{d} \quad (5)$$

$$D_{\mathrm{A}} = \left(\frac{x_{\mathrm{H}}}{D_{\mathrm{AH}}} + \frac{1-x_{\mathrm{H}}}{D_{\mathrm{AB}}}\right)^{-1} \quad (6)$$

Eq. (6), expressing the value of effective (pseudo binary) diffusion coefficient of transport limiting component A across a multicomponent gas–solid boundary layer, was theoretically derived in [6] from Maxwell–Stefan approach for reactions $A + nH_2 = B$ in case $D_{\mathrm{AH}} \approx D_{\mathrm{BH}} \gg D_{\mathrm{AB}}$ (assuming external transport control of reaction rate) and also experimentally confirmed in [6] for AMS and octene hydrogenation on a single catalyst pellet. Therefore, Chilton–Colburn analogy is justified (inspite of multicomponent problem), and conventional gas–solid heat/mass transfer empirical correlations may be used, for example, following [7] for spherical particles:

$$Sh = 2 + 0.6Re^{0.5}Sc^{0.33}$$

$$Nu = 2 + 0.6Re^{0.5}Pr^{0.33}$$

Calculation of the gas mixture conductivity is based on the assumption that $\lambda_{\mathrm{A}} = \lambda_{\mathrm{B}}$ and so the empirical method for binary nonpolar mixtures [8] is used:

$$\lambda = b\lambda_{\max} + (1-b)\lambda_{\min}; \qquad b = 0.32(1-x_{\mathrm{H}}) + 0.8x_{\mathrm{H}}$$

$$x_{\mathrm{A}} = \frac{P_{\mathrm{vap}}(T_0)}{P}; \qquad x_{\mathrm{H}} = 1 - x_{\mathrm{A}}$$

$$\lambda_{\max} = \lambda_{\mathrm{A}}(1-x_{\mathrm{H}}) + \lambda_{\mathrm{H}}x_{\mathrm{H}}; \qquad \lambda_{\min} = \left[\frac{x_{\mathrm{H}}}{\lambda_{\mathrm{H}}} + \frac{(1-x_{\mathrm{H}})}{\lambda_{\mathrm{A}}}\right]^{-1}$$

2.3. Analytical and numerical methods of finding model solution

System of three nonlinear Eqs. (1)–(3) includes three unknown variables T_{wet}, T_{dry}, f and also a set of parameters. It was interesting to study the influence of liquid flow rate G_{AMS} on the model solution, because extinction effect was experimentally found [4] when this parameter was gradually increased. Probably, the most poor determined parameter of this model is the coefficient of internal heat transfer α_{int}. The dependence of model solutions on this parameter also seems to be important. The clue to finding exact solution of the model Eqs. (1)–(6) is to consider G_{AMS} as the unknown variable but T_{wet} as the given parameter of the model. Variation of this parameter through some interval $T_0 < T_{\mathrm{wet}} < T_{\max}$ enables to find (step by step) the values of dry surface temperature T_{dry}, wet area fraction f and liquid flow rate G_{AMS}. The first step is to find the temperature rise (and the temperature value itself) of the dry part of surface from Eq. (2):

$$\Delta T_{\mathrm{dry}} = T_{\mathrm{dry}} - T_0 = \Delta T_{\mathrm{wet}}\left(\frac{\alpha_{\mathrm{int}}+\alpha}{\alpha_{\mathrm{int}}}\right) + \beta_{\mathrm{wet}}(C-C_0)\frac{H_{\mathrm{ev}}}{\alpha_{\mathrm{int}}} \quad (7)$$

After that the wet fraction f is found from Eq. (1):

$$f = \frac{\beta_{\mathrm{dry}}C_0Q_{\mathrm{p}} - \alpha\Delta T_{\mathrm{dry}}}{\alpha_{\mathrm{int}}(T_{\mathrm{dry}}-T_{\mathrm{wet}}) + \beta_{\mathrm{dry}}C_0Q_{\mathrm{p}} - \alpha\Delta T_{\mathrm{dry}}} \quad (8)$$

And at last the liquid flow rate is defined directly from Eq. (3). In such a way we get analytical solution in parametric form $T_{dry}(T_{wet})$, $f(T_{wet})$, $G_{AMS}(T_{wet})$. The suggested method enables to find both the stable and unstable branches of steady states, and also the critical (bifurcation) point, which divides them. But this analytical method cannot give information about the stability of steady states. So (in addition to previous analysis), direct numerical integration method was used to solve Eqs. (1)–(3) with the added unsteady terms (with time derivatives). If the initial conditions corresponded to dry pellet state, then unsteady solution displayed stabilization on the upper branch. For the sufficiently wetted initial pellet state unsteady solution was stabilized on the lower branch. When calculations were made for reverse time variable ($t = -t$), then solution approached the middle steady branch. Therefore, the upper and the lower steady state branches were found to be stable, the middle—unstable.

2.4. Discussion

The influence of the internal heat transfer coefficient α_{int} on the steady state curves is demonstrated on Fig. 2. Stable and unstable branches are connected by the bifurcation (extinction) points. Dry surface temperature rise (Fig. 2a) decreases, when the liquid flow rate increases. This is explained by growing of the heat flux from dry to wet surface. When the critical value of G_{AMS} is reached, the higher stable branch comes to extinction point. The physical meaning of this point is that the higher stable state disappears and the catalyst pellet suddenly becomes completely wet (with zero temperature rise).This horizontal branch is theoretically stable except the point $G_{AMS} = 0$. Unstable branches (dashed curves) divide the plain of initial conditions on two regions, attracted by the upper or the lower stable branch. It is clear that any disturbance of the lower steady state with $G_{AMS} = 0$ results in ignition. This conclusion is supported

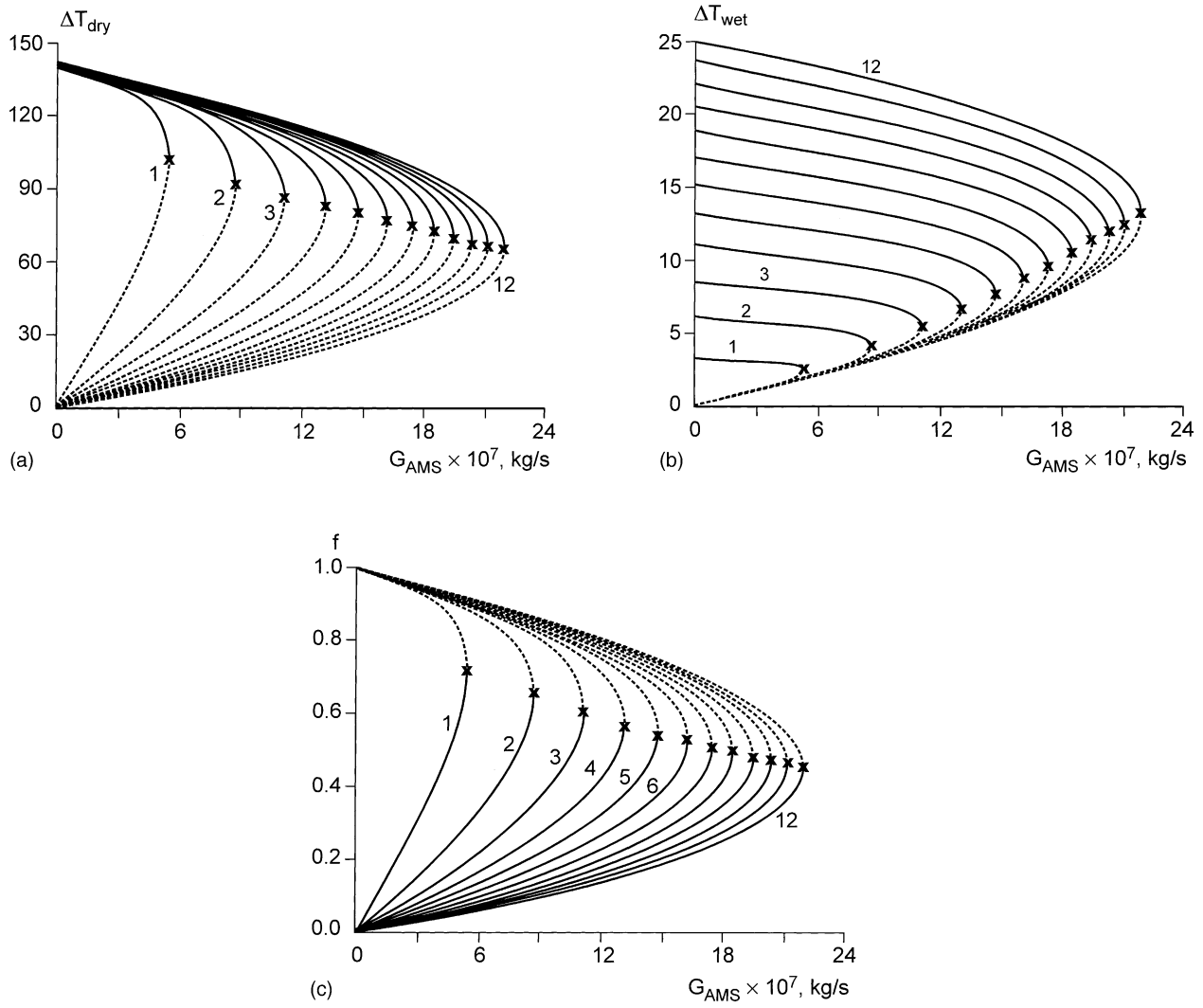

Fig. 2. Calculated steady state model solutions ΔT_{dry} (a), ΔT_{wet} (b), f (c) for increasing value of $\alpha_{int} = 25\,W/(m^2\,K)$ (curve 1), $\alpha_{int} = 50\,W/(m^2\,K)$ (2), ..., $\alpha_{int} = 300\,W/(m^2\,K)$ (12). Hydrogen flow is saturated by AMS vapor at $T_0 = 125\,^{\circ}C$. Critical points of extinction are marked by (x). Dashed curves correspond to middle unstable branches.

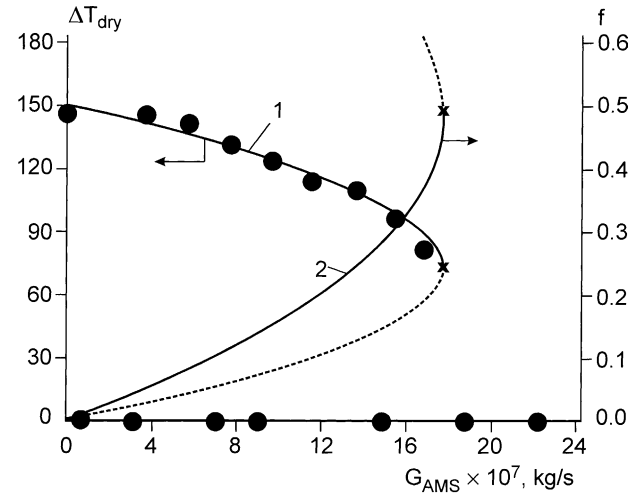

Fig. 3. Comparison of experimental data on pellet center temperature rise [4] for catalyst 0.5%Pd/C with model calculations ΔT_{dry} (1) and f (2) at $\alpha_{int} = 250\,W/(m^2\,K)$. The other conditions and notations are the same as in Fig. 2.

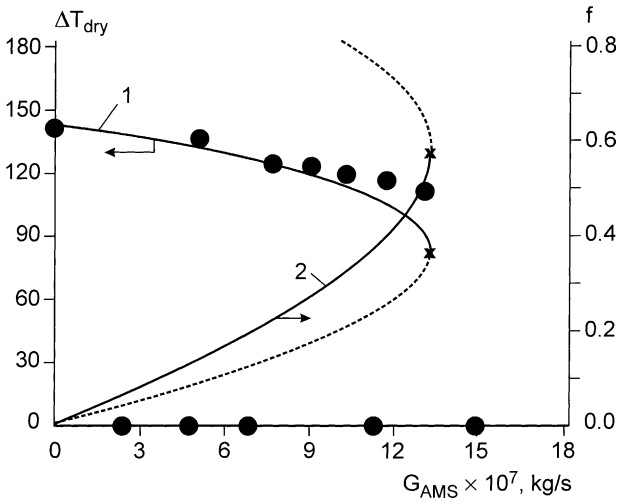

Fig. 5. Comparison of experimental data on pellet center temperature rise [4] for catalyst 15%Pt/Al_2O_3 (uniform Pt distribution) with model calculations ΔT_{dry} (1) and f (2) at $\alpha_{int} = 100\,W/(m^2\,K)$. The other conditions and notations are the same as in Fig. 2.

by experiments [4]. The model predicts extinction points on Fig. 2a, corresponding to the dry surface temperature level 190–270 °C, which is higher than AMS boiling temperature 165 °C. Extinction temperature of the wet surface is 130–150 °C (Fig. 2b). Wetted area fraction under conditions of extinction is approximately 0.45–0.70 (Fig. 2c). Figs. 3–6 show a comparison of experimental data [4] with the model (1)–(6) solutions. Rather good agreement was achieved for catalyst pellets Pd/C and Pd/Ti–Al (Figs. 3 and 4) if we take $\alpha_{int} = 250\,W/(m^2\,K)$, but Pt/γ-$Al_2O_3$ (Figs. 4 and 5) needs the lower values $\alpha_{int} = 67$–$100\,W/(m^2\,K)$. This discrepancy is easily explained by higher thermal conductivity value of carbon and Ti–Al porous support. It is important to note, that the experimental data for the catalyst pellets with

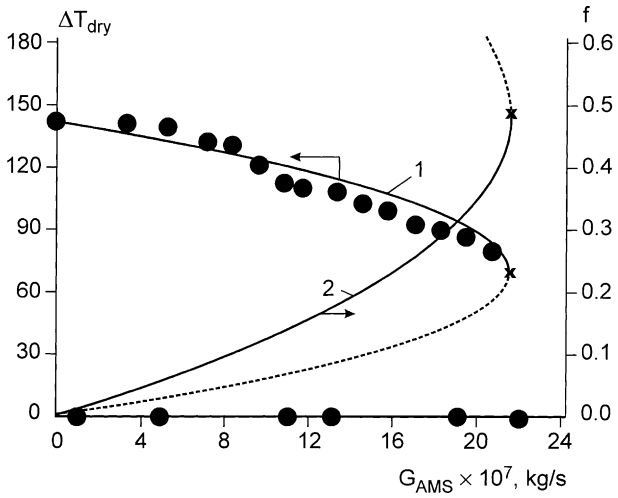

Fig. 4. Comparison of experimental data on pellet center temperature rise [4] for catalyst 3.5%Pd/Ti–Al with model calculations ΔT_{dry} (1) and f (2) at $\alpha_{int} = 250\,W/(m^2\,K)$. The other conditions and notations are the same as in Fig. 2.

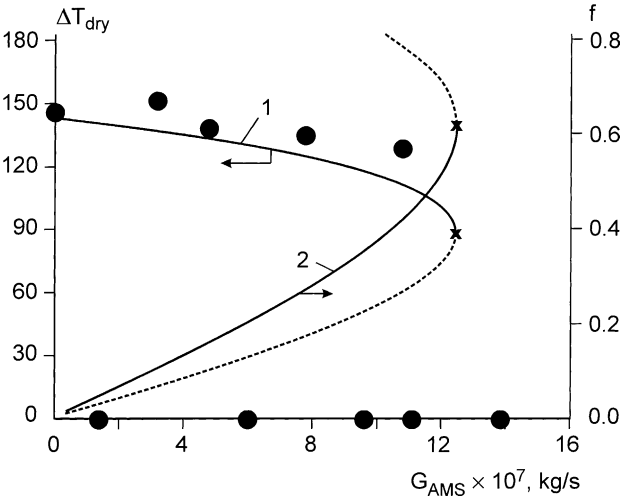

Fig. 6. Comparison of experimental data on pellet center temperature rise [4] for catalyst 15%Pt/Al_2O_3 (core-shell Pt distribution) with model calculations ΔT_{dry} (1) and f (2) at $\alpha_{int} = 67\,W/(m^2\,K)$. The other conditions and notations are the same as in Fig. 2.

uniform and core-shell types of active component distribution are very close and both are described by unique model (Figs. 5 and 6). The evident explanation is that the gas phase reaction takes place in the thin external layer of the pellet because of strong external transport limitation.

3. Case of 100% hydrogen flow

3.1. Physical assumptions

Catalyst pellet is isothermal and isobaric (Fig. 7). The imbibition rate per surface unit is large and, so, the external liquid film is negligible. Pellet structure is monoporous and

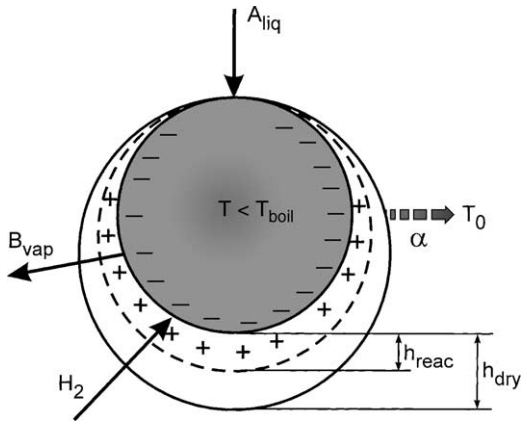

Fig. 7. Hypothetical catalyst pellet upper steady state branch in case if gas flow contains only hydrogen.

consequently a steep front divides the liquid filled and the gas filled intrapellet regions. The thickness of dry subsurface layer is small in comparison with pellet diameter, and the area of evaporation and reaction fronts is equal to the area of pellet external surface. Saturation conditions exist at the gas–liquid interphase front. Evaporation proceeds across the dry porous layer (internal diffusion resistance) and the gaseous boundary layer (external diffusion resistance). Free molecular diffusion of gas mixture through macropores is assumed. It is important to note that liquid phase reaction was taken into account in calculations (for the first model also), but its influence was found negligible owing to weak solubility of hydrogen under normal pressure (number He >10) and also its slow diffusion in liquid AMS. And this is the reason, why we excluded liquid phase reaction terms in both models.

3.2. Mathematical model of steady states

Heat balance for the catalyst pellet

$$W_{\text{reac}} Q_{\text{p}} = W_{\text{ev}} H_{\text{ev}} + (\alpha S + c_{\text{A}} N_{\text{AMS}})(T - T_0) \tag{9}$$

$$N_{\text{AMS}} = \frac{G_{\text{AMS}}}{M_{\text{AMS}}}$$

Evaporation rate for the pellet is equal to

$$W_{\text{ev}} = S\beta C_s = S\frac{D_{\text{ef}}}{h_{\text{dry}}}(C - C_s); \qquad C = \frac{P_{\text{vap}}(T)}{RT}$$

and one may exclude C_s and get

$$W_{\text{ev}} = \frac{S\beta(D_{\text{ef}}/h_{\text{dry}})}{\beta + (D_{\text{ef}}/h_{\text{dry}})} C(T) \tag{10}$$

$$D_{\text{ef}} = \frac{\varepsilon}{\tau} D_{\text{AH}}; \qquad \frac{\varepsilon}{\tau} = 0.1$$

Thickness of the dry subsurface layer, which is needed for 100% conversion of AMS vapor (if the kinetic rate is zero-order for H_2) is equal to

$$h_{\text{reac}} = \frac{N_{\text{AMS}}}{Sr}$$

Vapor phase AMS hydrogenation is known as structure insensitive reaction and we adopt intrinsic kinetic rate for Pd catalyst [1]

$$r = k_0 \exp\left(-\frac{E}{RT}\right) P_{\text{H}}^{0.8}; \qquad P_{\text{H}} = P - P_{\text{vap}}(T) \tag{11}$$

The overall rate of gas phase reaction is defined by three different expressions, depending on the pellet state:

(1) If the pellet is completely wet, i.e.

$$N_{\text{AMS}} > W_{\text{ev}}^{\max} = S\beta C(T) \tag{12}$$

then thickness of the dry layer and the reaction rate is zero

$$W_{\text{reac}} = 0; \qquad h_{\text{dry}} = 0 \tag{13}$$

In this case liquid AMS partially evaporates from the pellet external surface, the rest liquid simply trickles down the pellet. Another two pellet states assume complete AMS evaporation from the internal part of the pellet via diffusion across the dry subsurface layer.

(2) Thickness of the dry layer is not sufficient for 100% AMS conversion:

$$h_{\text{dry}} < h_{\text{reac}} \tag{14}$$

and, therefore, gas phase hydrogenation rate is lower than the evaporation rate

$$W_{\text{reac}} = Sh_{\text{dry}} r < Sh_{\text{reac}} r = W_{\text{ev}} \tag{15}$$

The corresponding value of AMS conversion is

$$X = \frac{h_{\text{dry}}}{h_{\text{reac}}} < 1 \tag{16}$$

(3) Complete AMS evaporation and conversion in the dry layer:

$$h_{\text{dry}} > h_{\text{reac}}; \qquad X = 1 \tag{17}$$

The gas phase reaction, the evaporation rate and the liquid flow rate are all equal in this case

$$W_{\text{reac}} = W_{\text{ev}} = N_{\text{AMS}} \tag{18}$$

3.3. Method of solution

The graphical-analytical method was used for construction of model solutions. It is convenient to demonstrate this method with the help of Fig. 8a. Part FB of the lower stable branch curve IFB correspondence to the completely liquid filled pellet. Liquid AMS feed is partially vaporized from the pellet surface, the rest liquid is trickling down. Pellet temperature is lower than hydrogen flow temperature and is practically independent on the liquid flow rate. The value of pellet temperature may be defined from the Eqs. (9), (12) and (13) from the following relation

$$S\beta C(T) H_{\text{ev}} = (\alpha S + c_{\text{A}} N_{\text{AMS}})(T - T_0) \tag{19}$$

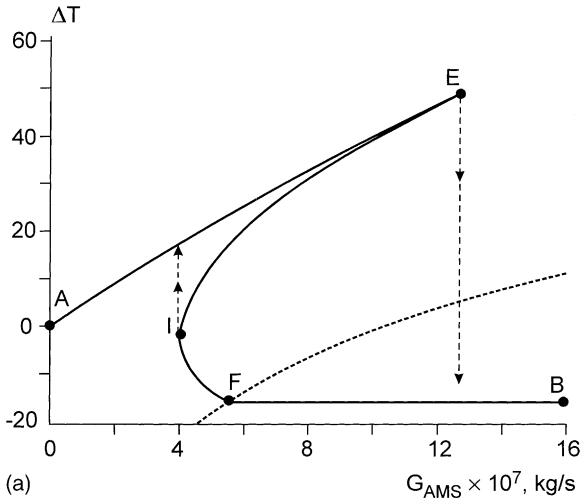

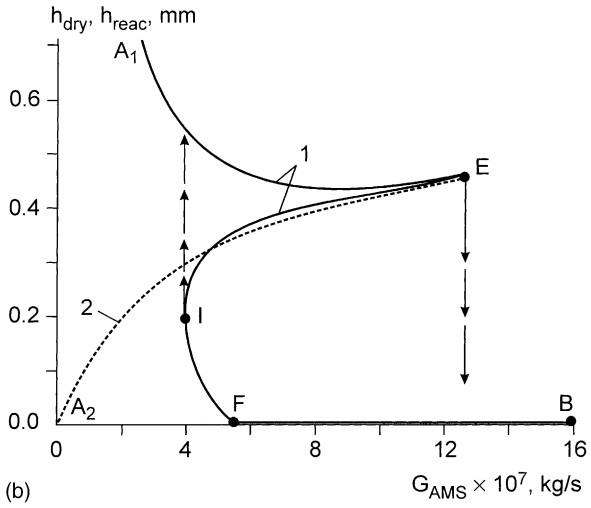

Fig. 8. Hysteresis type behavior modeling: (a) ΔT; (b) h_{dry} (curve 1) and h_{reac} (curve 2). Hydrogen gas flow at $T_0 = 80\,^{\circ}C$. AE, A_1E, A_2E—upper steady state branches; IFB, lower branch; IE, middle branch; *E*, extinction point; *I*, ignition point, *F*, point of complete wetting.

The point *F* corresponds to the boundary on which the vaporization rate for the completely wet pellet is exactly equal to the liquid flow rate. The equation for this boundary (dotted curve on Fig. 8a) is

$$N_{AMS} = S\beta C(T) \tag{20}$$

Part FE corresponds to complete evaporation but partial AMS vapor conversion across the dry layer (Eqs. (14)–(16)). The construction of FE-curve is made by the following method. Pellet temperature *T* is considered as the known parameter, but the liquid flow rate N_{AMS}—as unknown variable. Taking into account the condition of complete evaporation

$$W_{ev} = N_{AMS} \tag{21}$$

Eq. (10) is transformed to

$$h_{dry} = \frac{D_{ef}}{\beta}\left[\frac{S\beta C(T)}{N_{AMS}} - 1\right] \tag{22}$$

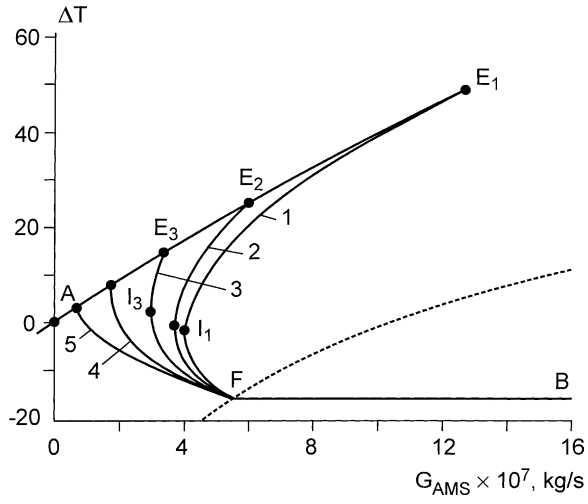

Fig. 9. Hysteresis type dependence ΔT on G_{AMS} under decrease of pellet catalytic activity: $k_1 = k_0$, $k_2 = 0.8k_0$, $k_3 = 0.45k_0$, $k_4 = 0.2k_0$, $k_5 = 0.07k_0$. Hydrogen gas flow at $T_0 = 80\,^{\circ}C$. E_1, E_2, E_3—extinction points. I_1, I_2, I_3—ignition points. Value k_0 corresponds to Fig. 8.

With the usage of Eqs. (15) and (21) the reaction rate may be written as

$$W_{reac} = S\frac{D_{ef}}{\beta}\left[\frac{S\beta C(T)}{N_{AMS}} - 1\right] r(T) \tag{23}$$

Making the substitution of the Eqs. (21) and (23) into Eq. (9) and multiplying it by N_{AMS}, one can get the second-order equation for unknown N_{AMS}:

$$a_2 N_{AMS}^2 + a_1 N_{AMS} - a_0 = 0 \tag{24}$$

$$a_2 = [H_{ev} + c_A(T - T_0)] > 0$$

$$a_1 = \left[Q_p \frac{D_{ef}}{\beta} r + \alpha S(T - T_0)\right] > 0$$

$$a_0 = Q_p SrC > 0$$

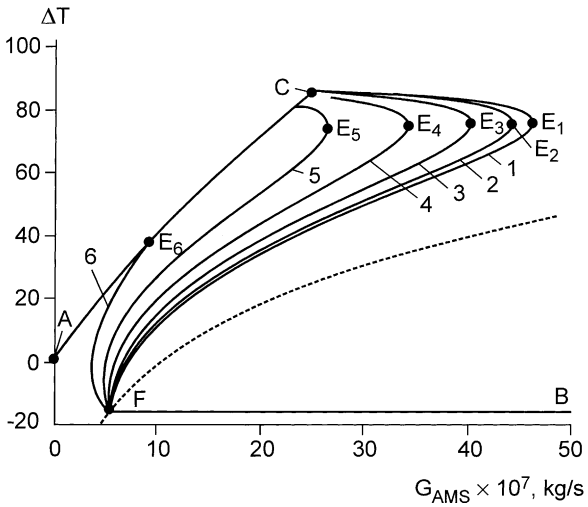

Fig. 10. Hysteresis type dependence ΔT on G_{AMS} under increase of pellet catalytic activity: $k_1 = 7k_0$, $k_2 = 6k_0$, $k_3 = 4.7k_0$, $k_4 = 3.3k_0$, $k_5 = 2k_0$, $k_6 = k_0$. The other notations are the same as in Fig. 9.

Physical meaning has the only one (positive) of two roots of Eq. (24), which defines FE-curve on Fig. 8a:

$$N_{\mathrm{AMS}} = \frac{-a_1}{2a_2} + \sqrt{\left(\frac{a_1}{2a_2}\right)^2 + \frac{a_0}{a_2}} \tag{25}$$

FI-curve continues the lower stable steady state branch IFB. The ignition point (I) marks the transition to the upper steady state branch AE, when the liquid flow rate is decreasing. So, the IE-curve is the middle steady state branch. The upper branch (curve AE) is defined by Eq. (9) under conditions (17) and (18):

$$\Delta T = T - T_0 = \frac{N_{\mathrm{AMS}}(Q_{\mathrm{p}} - H_{\mathrm{ev}})}{(c_{\mathrm{A}} G_{\mathrm{AMS}} + S\alpha)} \tag{26}$$

The extinction point E marks the transition to the lower branch, when the liquid flow rate is increasing. This point is defined as the intersection of IE and AE curves.

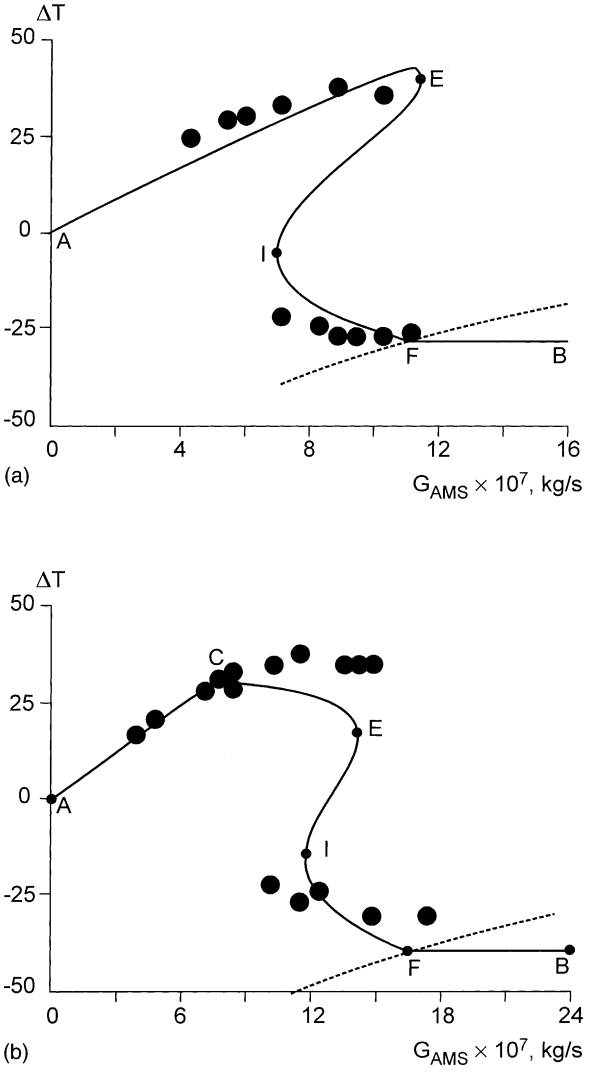

Fig. 11. Comparison of experimental data on pellet center temperature rise [4] for catalyst 15%Pt/Al_2O_3 (uniform Pt distribution) with calculated ΔT. Hydrogen gas flow at $T_0 = 110\,^{\circ}\mathrm{C}$ (a), $T_0 = 132\,^{\circ}\mathrm{C}$ (b).

3.4. Discussion

Hysteresis dependence of dry layer thickness h_{dry} and complete conversion thickness h_{reac} on liquid flow rate G_{AMS} is shown on Fig. 8b. The influence of decreasing catalytic activity is demonstrated in Fig. 9. The ignition point shifts slightly to lower values of liquid flow rate (I_1–I_2–I_3). The extinction point also shifts in the same direction, but more significantly (E_1–E_2–E_3). If catalyst activity is sufficiently low, than hysteresis and multiplicity disappear. The influence of increasing catalytic activity is demonstrated in Fig. 10. If activity is sufficiently high, then the point of ignition is placed very close to point F (where the pellet drying begins). Extinction point shifts far to the region of high liquid flow rates. The pellet temperature approaches AMS boiling temperature 165 °C (near the point C). Additional branch CE of the higher steady state branch AE arises. In this case, extinction is explained by the decrease of hydrogen partial pressure and, consequently, the decrease of intrinsic kinetic rate of gas phase hydrogenation. Finally, the comparison of experimental data [4] with modeling is presented in Fig. 11.

4. Conclusions

Physical and mathematical models with lumped parameters have been developed, which explain experimental critical phenomena on a single catalyst pellet. The mechanism of critical phenomena is based on the interaction between the endothermic process of liquid reactant evaporation and the vapor phase exothermic reaction. The results of mathematical modeling confirmed our previous experimental observations, that poorly wetted catalyst pellets in a trickle-bed reactor may undergo “ignition”, resulting in high flow-pellet temperature rise. If a catalyst pellet is ignited, it is not easy to return it to a normal completely wetted state, because the significantly higher liquid flow rates are necessary for its “extinction” (hysteresis phenomena). Meanwhile, the critical extinction/ignition values of linear liquid velocity for catalyst pellets, considered in this study (0.05–0.10 mm/s) are significantly lower than the values [9] in industrial trickle-bed reactors (>3–4 mm/s). Therefore, if liquid distribution is not significantly nonuniform in industrial reactors, then no pellets may undergo “ignition”. Thus arises the problem of scaling up (for critical conditions) from pellet level to catalyst bed. Nevertheless, the important conclusion is that the boundary of hot spot zones in trickle-bed reactor may consist of poorly wetted ignited pellets and be rather stable for liquid flow variations. Hysteresis phenomena strikes the danger of reactor start-up from low liquid flow rates. Perhaps, the most reliable way to provide thermal safety of trickle-bed reactor (which indeed is often used in industry) is to dilute inlet liquid feed with outlet product so, that heat of mixture evaporation would exceed possible heat generation (under its complete conversion). In the last case the considered critical phenomena becomes thermodynamically

impossible. Unfortunately, it is not usually easy to predict which catalytic side reactions may occur for real complex hydrogenated mixtures. But excessive dilution often leads to poor reactor productivity. May be, ignited catalyst pellets are not so dangerous, if they are distributed in trickle-bed among the "normal" ones. Moreover, such moderately hot pellets may provide sharp increase of reactor productivity. The intriguing question still remains, how separate ignited pellets may be self-organized into hot spots with the following expansion in reactor scale, resulting in runaway.

Table of model parameters

Parameter	Value
Q_p (J/mol)	109×10^3
H_{ev} (J/mol)	43×10^3
c_A (J/(mol K))	200
M_{AMS} (kg/mol)	118
S (m^2)	1.25×10^{-4}
E (J/mol)	37.8×10^3
R (J/(mol K))	8.31
d (mm)	5
D_{AB} (m^2/s)	5×10^{-6}
D_{AH} (m^2/s)	7.5×10^{-5}
λ_H (W/(m K))	0.254
λ_A (W/(m K))	0.024
P^* (N/m^2)	1.337×10^{10}
P (N/m^2)	10^5

Acknowledgements

The authors wish to thank the Netherlands Organization for Scientific Research (NWO) for financial support and are grateful to Prof. K.R. Westerterp and Dr. A. Kronberg for their interest to this research.

References

[1] A.H. Germain, A.G. Levebvre, G.A. L'Homme, Experimental study of catalytic trickle-bed reactor, Adv. Chem. Ser. 133 (1974) 164.
[2] J. Ruzicka, J. Hanika, Partial wetting and forced reaction mixture transition in a model trickle-bed reactor, Catal. Today 20 (1994) 467.
[3] P.C. Watson, M.P. Harold, Rate enhancement and multiplicity in a partially wetted and filled pellet: experimental study, AIChE J. 40 (1994) 97–111.
[4] A.V. Kulikov, N.A. Kuzin, A.B. Shigarov, V.A. Kirillov, A.E. Kronberg, K.R. Westerterp, Experimental study of vaporization effect on steady state and dinamic behaviour of catalytic pellets, Catal. Today 66 (2001) 255–262.
[5] M.P. Harold, Bimolecular exothermic reaction with vaporization in the half-wetted slab catalyst, Chem. Eng. Sci. 48 (1993) 981–1004.
[6] V.A. Kirillov, N.A. Kuzin, A.V. Kulikov, B.N. Lukyanov, V.M. Hanaev, A.B. Shigarov, Study of external diffusion regime of gas phase hydrocarbons hydrogenation on a catalyst pellet, Theor. Found. Chem. Eng. 34 (2000) 526–535 (in Russian).
[7] G.A. Hugmark, Mass and heat transfer from rigid spheres, AIChE J. 13 (1967) 1219.
[8] R.C. Reid, J.M. Prausnitz, B.E. Poling, Properties of Gases and Liquids, 4th Edition, McGraw-Hill, New York, 1987.
[9] Y. Jiang, M.H. Al-Dahhan, M.P. Dudukovic, Statistical characterization of macroscale multiphase flow textures in trickle-beds, Chem. Eng. Sci. 56 (2001) 1647–1656.